Controlling the melt dripping of poly(ethylene terephthalate) fabrics by tuning the ionic strength of layer by layer assembled polyhedral oligomeric silsesquioxane and sodium montmorillonite coatings

Alessandro Di Pierro[1], Jenny Alongi[2], Alberto Fina[1], Guido Saracco[3], Federico Carosio[1]

Dipartimento di Scienza Applicata e Tecnologia, Politecnico di Torino, Alessandria Campus,

Via Teresa Michel 5, 15121 Alessandria, Italy

2 Dipartimento di Chimica, Università degli Studi di Milano, Via Golgi 19, 20133 Milano, Italy

3 Center for Space Human Robotics @ PoliTo, Istituto Italiano di Tecnologi A, C.so Trento, 21, Torino, Italy

*Corresponding author:

e-mail address:

Abstract

This work deals with the Layer by Layer assembly of inorganic coatings made of octaammonium POSS and sodium montmorillonite clay on polyester (PET) fabric employing a semi industrial approach and investigating the effects of ionic strength on the achieved flame retardancy properties. Coating growth followed by infrared spectroscopy points out that the inclusion of NaCl results in thicker coatings. 0.1 M NaCl is found to promote the highest adsorption at each deposition step. High ionic strength coatings yielded more homogeneous and thicker coatings when deposited on PET. Thanks to the increased thickness and better surface coverage, the same coatings efficiently suppressed the melt dripping phenomenon and significantly slowed down flame spreading rate in horizontal flammability tests. Moreover, these performances were maintained after 1 hour washing at 70°C. By cone calorimetry treated fabrics showed a strong reduction in the combustion kinetics by nearly halving the peak of heat release rate. This paper provides an important insight on the viability of tuning ionic strength when depositing LbL coatings on fabrics employing industrial-like processes.

Introduction

Nowadays the production of synthetic fibers and fabrics, like polyesters and polyamides, has become the first around the world of textile industry surpassing the production of natural ones.[1] This massive production and use in many fields such as furniture, clothing industry, automotive, sport equipment and many others surrounded us with comfortable, cheap yet fast burning and melting materials.[2] The presence of such fast burning materials in everyday life increases the risk of fire ignition and development. In order to prevent this occurrence, the consolidated practice is to improve the fire proprieties of polymers using chemicals known as flame retardants (FRs). FRs are normally employed either by bulk addition in melt-blending processing or, less commonly, by copolymerization of intrinsically designed flame retarded monomers or polymers.

In past decades many of the effective solutions for flame retarded materials relied on the chemistry of brominated or halogenated compounds; unfortunately, in recent years legislators have stimulated the research of safer alternatives due to perceived health and environment hazards related to such chemicals. Indeed, some of the traditional FRs have been found to be toxic [3] and persistent in the environment, [4] eventually ending up in the food chain. [5]A possible solution is represented by the so called surface approach, a recent trend that aims at the confinement of safe flame retardants on the surface rather than in the bulk of the polymer by means of nanotechnology.[6 7] This is a change in perspective when considering the approach to fire protection and it's related to the key role played by the surface during combustion. Indeed, during combustion, the heat from the flame is transmitted through the surface to the bulk; simultaneously, the bulk thermally degrades and produces combustible volatiles that diffuse towards the surface feeding the flame in a self-sustained process. [8] Thereby, by modifying the interface between the condensed matter and the flame it is possible to control heat and mass transfers and hinder the burning behavior of a polymer. [9]

In this scenario the Layer by Layer (LbL) technique turned out to be a valuable tool for the deposition of multi-layered coatings with flame retardant functionalization on fabrics, [10] foams [11]

[12] [13] [14] and films. [15] [16] Beside flame retardancy the LbL has been adopted in other research fields such as sensors, [17] enzymes, [18] drug delivery control, [19] carrier systems [20] and more. [21] The LbL is a relatively simple technique; its fundamentals can be dated back to the 60's with the experimental evidence about structures assembled by the alternate deposition of oppositely charged particles. [22] Then, at the beginning of the 90's, this basic concept was extended by Decher to the self-assembly of oppositely charged polyelectrolytes and the LbL became a general approach for the fabrication of multicomponent films on solid substrate. [23] [24] In a raw description, the LbL consists in the stepwise selective adsorption of different interacting species on a substrate. The interactions are due to electrostatic attraction, [25] hydrogen bonding, [26] ionic-covalent bonding [27] or donor-acceptor coupling. [28] All these interactions allow for the layered self-adsorption of the selected species from dilute suspensions (or solution). Following this route it is possible to obtain complex multi-layered structures with unlimited composition possibilities. Another key point of the Lbl, that makes this approach even more attractive, is represented by the possibility of tuning the physical/chemical characteristics of the deposited coating by changing the deposition parameters. However, as far as the deposition of flame retardant coatings is concerned, there are only few studies that focus on the effect of the deposition parameters on the achieved fire protection performance. Recently, we showed how pH and molecular weight of the selected polyelectrolytes can influence the burning behavior of cotton fabrics but, [29] to the best of our knowledge, there are no studies evaluating the effect of ionic strength on the flame retardancy properties LbL coatings. The ionic strength is one of the typical tuning parameter for LbL depositions; by increasing the ionic strength it is possible to increase the film thickness and also it's adhesion to the substrate. [30] [31] [32]

Thereby, the study of this parameter is of potential interest for an industrial application as thick and more performing FR coatings could be deposited with a reduced number of deposition steps.

In this paper we are addressing the deposition of a FR LbL coating consisting of polyhedral oligomeric silsesquioxane (POSS) and sodium montmorillonite (MMT) on PET fabrics

investigating the effects of ionic strength on the final performances. While both POSS and MMT present recognized flame retardant characteristics when employed in surface approach to flame retardancy, [33] [34] their combination in a LbL assembly has never been attempted before. Moreover, the effects of LbL coatings on the FR properties of PET and more generally synthetic fibers have not been studied as heavily as for the other cellulosic fabrics. The reasons have to be searched in the different burning behavior of the two categories. Indeed, due to their thermoplastic nature synthetic fibers can melt and vigorously drip during combustion thus compromising the stability and efficiency of the deposited LbL coating. This behavior poses additional and strong scientific challenges as the deposited coating has to be extremely efficient in order to obtain a substantial FR effect.

First, the coating growth at different ionic strengths has been followed by infrared spectroscopy. Then, the best growing conditions, along with the unmodified assembly, have been selected and transferred to the PET substrate employing a finishing-like process as reported in Figure 1.

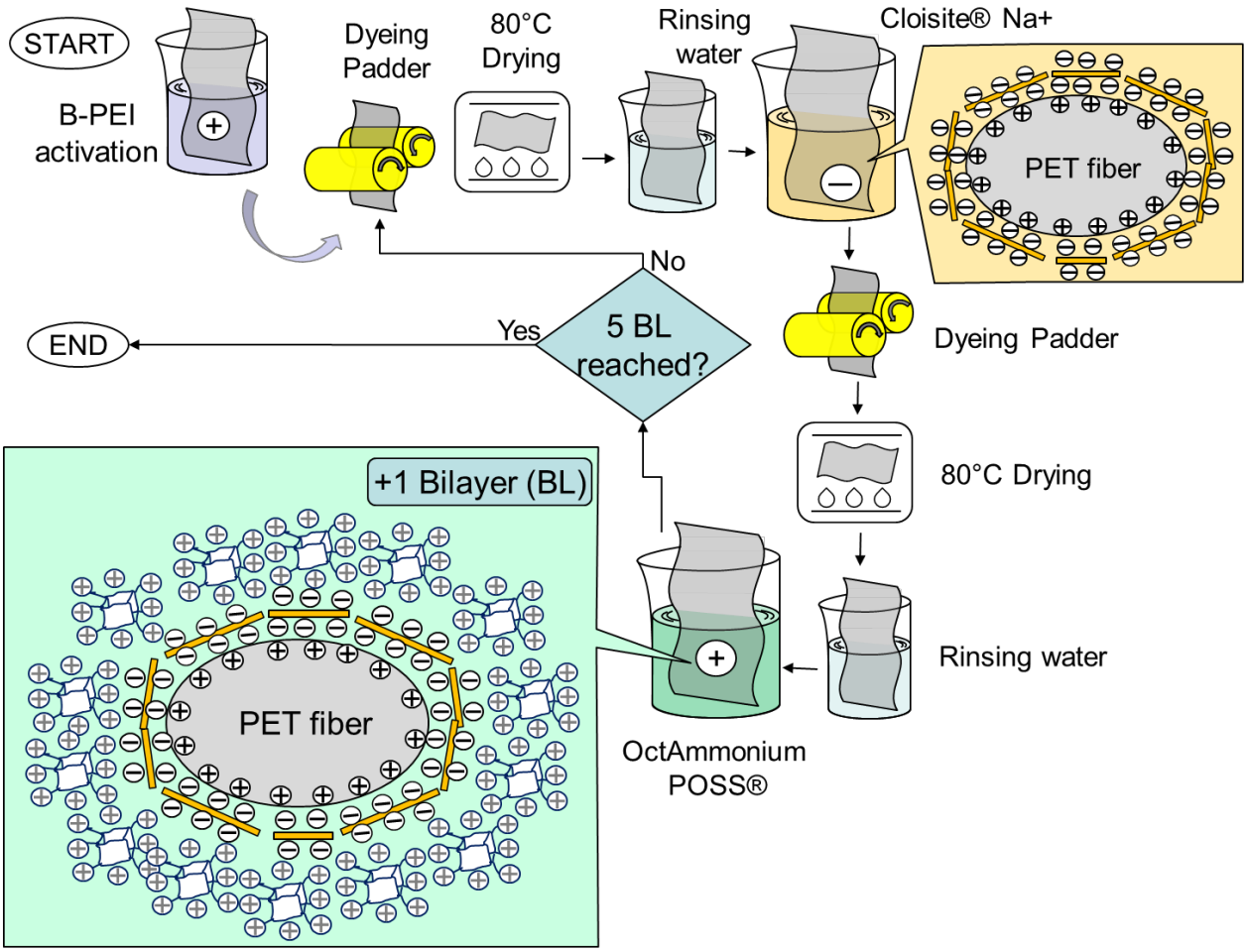

Figure 1 Schematic representation of the LbL process adopted in the present study. The PET fabric is primed by a branched poly(ethylene imine) and then alternatively dipped in Cloisite Na+ suspension (negative) and OctAmmonium POSS solution (positive) until 5 BL are reached.

The use of a semi industrial approach as reported in Figure 1 is of scientific interest and challenging at the same time. Indeed, by simulating a process that occurs in practical application it is possible to evaluate the viability of the proposed approach in a more relevant and pertinent way with respect to the standard dipping procedure commonly adopted in LbL studies. On the other hand, the high deformations imparted to the coating during the padding processes might compromise the deposition of the coating to the point of making it impracticable. This is particularly important for

LbL assemblies at high ionic strength since in the wet and swelled state the interactions between the components are weaker and thus the coating is more likely to suffer from strong deformations.[35]

Treated fabrics have been imaged with field emission scanning electron microscopy (FE-SEM) and probed by FTIR-ATR spectroscopy in order to evaluate the changes in morphology and surface chemical composition. The thermal and thermo-oxidative stability have been assessed by termogravimetric analysis (TGA) in nitrogen and air, respectively. The flame retardancy properties have been evaluate by means of reaction to an applied flame (horizontal flame spread) and impinging heat flux (cone calorimetry). Finally, the best formulation has been selected for a simple washing test in order to obtain preliminary information concerning the durability of the deposited coatings.

Experimental

Materials

The polyester fabric with a grammage of 55g/m^2 was purchased from Fratelli Ballesio S.r.l. (Turin, Italy). The surface has been activated with an aqueous solution of 0.1% in weight of branched poly(ethylene imine) (BPEI, Mw ~25000 by Laser Scattering, Mn ~10000 by GPC (Gel Permeation Chromatography) as reported by the producer). The pH of the solution was kept unaltered at pH=10 after 1h stirring. The sodium montmorillonite (Southern clays, US), was used for preparing 1%wt water suspensions that were kept under magnetic stirring for 24h and then centrifuged for 5 minutes at 4400 rpm to remove the bigger and unsuspended particles yielding a final concentration of 0.7%. The OctaAmmonium POSS was purchased from Hybrid Plastics (Hattiesburg, MS) and solubilized at 1% in weight. This product is highly soluble in water and no further operations are needed. The NaCl used to change the ionic strength to the aqueous solutions was purchased from Sigma Aldrich with a purity at least 99.5% and used without further treatments. Solutions and suspensions were prepared using 18.2 M deionized water supplied by a Q20 Millipore system (Milano, Italy).

LbL deposition

Si wafers: In order to prime the surface, the Si wafer or PET fabric were dipped 2 minutes in the 0.1% in weight B-PEI solution before the deposition cycles. This step promotes the LbL coating growth and adhesion, as already described in the literature. Then, the growth of three different ionic strength samples has been observed from transmission infrared spectroscopy on Si wafers; a system made of Cloisite Na+ and OctaAmmonium POSS without NaCl in solution and two systems with the addition of 0.05 M and 0.10 M of NaCl in every vessel (including the rinsing ones). After the activation step with BPEI the Si wafer were alternately immersed into the negatively (MMT) and the positively (POSS) charged solutions (2 min dipping); after each adsorption step, the excess solution was removed by static washing (2 min) and compressed air.

PET fabrics: similarly to Si wafer, the PET fabrics were dipped 2 minutes in the 0.1% in weight BPEI solution. Then, the fabrics were alternately dipped into the negatively (MMT) and the positively (POSS) charged solutions (2 min dipping) following the procedure described in Figure 1. In between each adsorption step, the fabrics were squeezed using a Padder model FL300 produced by Gavazzi s.r.l (Bergamo, Italy) and dried in a convection oven at 80°C for 5 min, mimicking a finishing industrial treatment. Then, before moving to the next deposition solution the fabrics were washed by 2 minutes dipping in water bearing the same ionic strength of the one employed for the deposition. The process was repeated in order to deposit a total of 5 BL without modifying the ionic strength and in the presence of 0.1 M NaCl. The corresponding samples were codes as 5 BL and 5 BL 0.1 M NaCl. The final weight gain on fabrics was approximately 1.2% for the system without NaCl and 2.0% at 0.1M of NaCl.

Characterization

Fourier transformed infrared spectroscopy: the growth of the LbL assembly on a silicon wafer substrate was followed at room temperature using a Frontier FT-IR spectrophotometer (16 scans and 4cm^{-1} resolution, Perkin Elmer). IR spectra in the range 4000-400 cm^{-1} were acquired after each bilayer was built.

Fourier transformed infrared spectroscopy in attenuated total reflectance: spectra were collected at room temperature in the range 4000-700cm^{-1} (16 scans and 4cm^{-1} resolution) using a Frontier FT-IR/FIR spectroscopy (Perkin Elmer, Italy) equipped with a germanium crystal (nominal depth of penetration 600 nm, as stated by the Producer).

Field Emission-Scanning Electron Microscopy: the surface morphology of untreated and LbL-coated fabrics was observed using a Field Emission Scanning Electron Microscope (FESEM), model Merlin from Zeiss. Samples were cut in 10x10 cm^2 pieces, pinned up to conductive adhesive tapes and chrome-metallized prior to imaging.

Thermogravimetric analysis: TGA were performed on a thermogravimetric balance TGA-Q500 from 50 to 800°C + (using heating rate of 10°C/min) in both nitrogen and air (gas flux 60mL/min). 10±0,5 mg samples were placed in open alumina pans. From TG and dTG curves, the collected data were T_{onset} (temperature at 5% weight loss), T_{max} (temperature at maximum weight loss) and the residue at 800°C.

Horizontal flame spread: The flammability test has been evaluated in horizontal configuration following the UL 94 HB testing scheme with a 45°degrees inclination on the longer axe. The specimen (size: 150mm x 50mm) was ignited from its short side by a 20mm methane flame (flame application time: 3s). During the test, parameters such as afterflame time (time of flame persistence after the ignition source has been removed, in seconds), average burning rate (mm/s), occurrence of melt dripping and cotton ignition and final residue (%) were collected.

Cone Calorimetry: a cone calorimeter from FTT (Fire Testing Technology) according to the standard ISO 5660 was employed to investigate the combustion behavior of the fabrics. Specimens were wrapped in aluminum foil leaving the upper surface exposed to the cone resistance and placed on ceramic backing board at a distance of 25 mm from cone base. Due to the lightweight nature of the fabric this test has been performed on 6 plies stacked together and hold in position with a metallic grid. The square samples of 6 plies 100x100mm^2 were irradiated by a heat flux of 35kW/m^2 in horizontal configuration, following the procedure described in literature. [36] The registered parameters were: Time To Ignition (TTI, seconds), the Heat Release Rate (HRR and its peak pkHRR, kW/m^2), the Total Heat Release (THR, MJ/m^2), the Total Smoke Released (TSR, m^2/m^2) and final mass residue in percent. The test was repeated 3 times for each formulation in order to improve reproducibility.

Results and discussion

Coating growth by FTIR

The coating growth has been observed through transmission Infrared spectroscopy on Si wafers. First of all, the spectrum of each layer constituent has been evaluated (supplementary material Figure 1). Neat POSS shows characteristics peaks ascribed to Si-O-Si cage vibrations in the 1200-1000 cm^{-1} range with the most intense peak at 1132 cm^{-1} ascribed to Si-O stretching; moreover, signals related to NH_3^+ asymmetric and symmetric stretching vibrations can be found at 1612 and 1510 cm^{-1}, respectively. [37] For what concerns MMT, characteristics signals are found at 1043 cm^{-1} (Si-O stretching vibration), 520 cm^{-1} (Si-O-Al bending vibration) and 464 cm^{-1} (Si-O-Si bending vibration). [38] When the two components are LbL assemble a steady coating build-up is observed. Figure 2 reports the elaboration of IR signals of the POSS and MMT system grown on a silicon substrate with no added salt and the intensity plot of the peak at 1043 cm^{-1} as a function of BL number for each tested system.

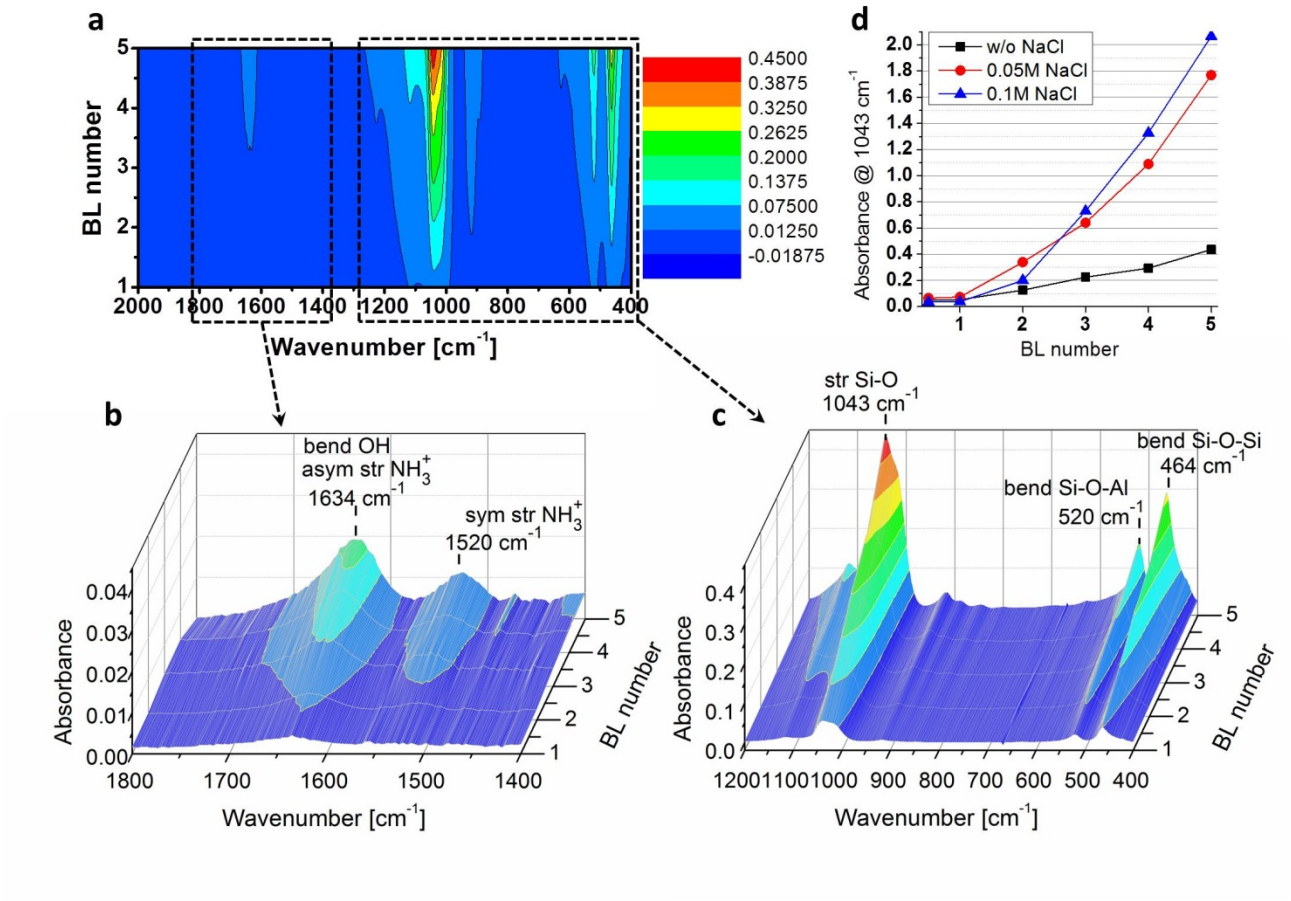

Figure 1. Coating growth of 5 bilayers (BL) sodium montmorillonite/octaammonium POSS followed by FTIR: contour plot of IR absorption in the 2000-400 cm^{-1} (a), 3D plot absorptions in the 1800-1400 (b) and 1200-400 (c) cm^{-1} and 1040 cm^{-1} signal intensity as a function of BL number at different ionic strengths (d).

As reported in figure 2, when assembled at unmodified ionic strength the IR signals of the LbL coating increase as a function of the BL number. The most intense peaks are found in the 1200-400 cm^{-1} region and are mainly ascribed to MMT Si-O stretching and Si-O-Al/Si-O-Si bending vibrations (Figure 2 c). While MMT signals overlaps with POSS ones in the 1200-1000 cm^{-1} range, the presence of the positively charged component is clearly pointed put but the signals associated to NH_3^+ asymmetric and symmetric stretching vibrations found in the 1800-1400 cm^{-1} region (Figure 2b). Furthermore, it is worth pointing out that these latter signals are shifted towards higher wavenumbers with respects of pure POSS (compare Figure S1 with Figure 2b) as a consequence of

the ionic interactions established with the negatively charged surface of MMT during the LbL assembly. The intensity of the peak at 1043 cm^{-1} reported in Figure 2 d as a function of BL number suggests a linear growth of the POSS/MMT system deposited without salt addition. On the other hand when the ionic strength is modified with the inclusion of 0.1 and 0.05 M of NaCl the growth regime of the assembly remains linear but it allows for the deposition of thicker coatings. Indeed, by increasing the ionic strength of the solutions it is possible to increase the amount of POSS and MMT deposited at each step as demonstrated by absorbance vs BL number plots in Figure 2d. From data reported in Figure 2d it seems that the inclusion of 0.1 M NaCl provides the best growing conditions; thus this system, along with the unmodified one, has been chosen for the deposition on PET fabrics.

Coating characterization on PET fibers

The selected coatings were transferred to PET fabrics exploiting the procedure described in materials and methods. Then the changes in surface morphology and chemistry of unmodified and LbL coated fabrics have been evaluated by means of FE-SEM and ATR analyses, respectively. Figure 3 reports collected micrographs and spectra.

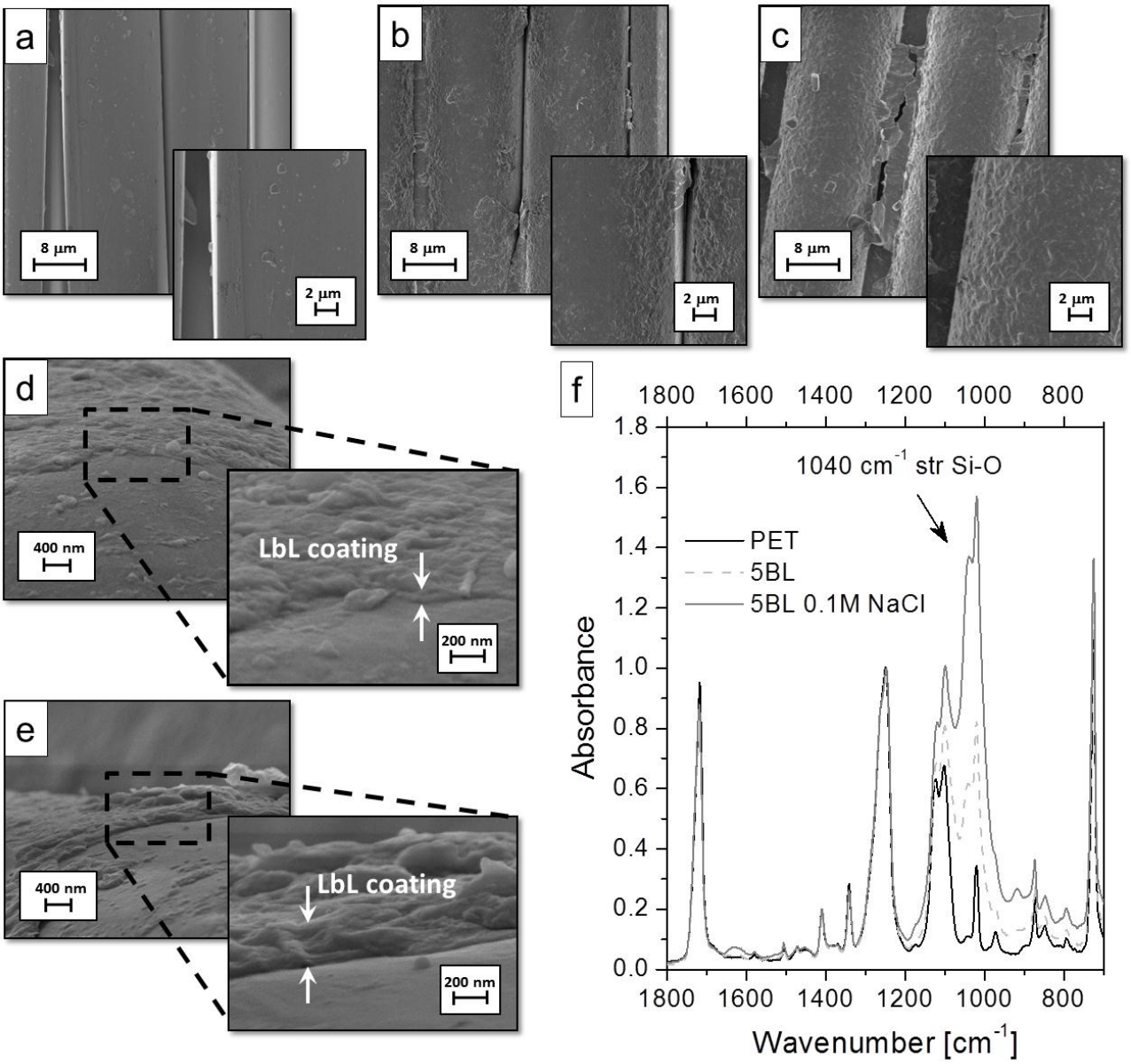

Figure 2. FESEM micrographs of unmodified and LbL treated PET fabrics: neat PET (a), 5BL (b), 5BL 0.1M NaCl (c); coating cross section on 5BL (e) and 5BL 0.1M NaCl and (f); ATR spectra.

Unmodified PET fibers show a regular and smooth surface typical of synthetic fibers (Figure 3a). When the fabrics are LbL treated a clear change in surface morphology can be easily detected (Figure 3b and c); the presence of the coating is evidenced by an increased roughness mainly ascribed to staked MMT nanoplatelets. Moreover, regardless of the adopted ionic strength the LbL deposition was found able to completely cover the surface of PET fibers. Differences between the two adopted deposition conditions are evidenced by a more homogeneous fiber coverage and the formation of bridging phenomena between adjacent fibers only occurring at 0.1 M NaCl (compare

Figure 3 b and c). Cross section micrographs further point out the difference in thickness between the two systems; indeed, from Figure 3d and e it is apparent that the coating built at higher ionic strength is the thicker one. This is also confirmed by ATR spectra (Figure 3) where the signal ascribed to Si-O stretching vibration is more intense for 5 BL 0.1 M NaCl. From the collected characterization it is possible to conclude that both system can efficiently cover the surface of PET fibers and yield a homogeneous coating after the deposition of 5 BL. As studied on model Si wafer surface, the increase of ionic strength results in the deposition of a thicker coating also on PET fabrics. This latter finding is important as it demonstrates that the high deformations imparted to the coating during the padding processes do not compromise the stability of the coating. The add-on evaluated by weighting the fabrics before and after the LbL deposition was found to be 1.2 and 2% for 5 BL and 5 BL 0.1 NaCl, respectively.

Thermal characterization

The thermal and thermo-oxidative stability of untreated and LbL treated PET fabrics were investigated by TGA both in nitrogen and air atmosphere. The aim is to obtain basic degradation information useful for the interpretation of possible effects of the LbL coating on the char production mechanisms of PET and its high temperature oxidation. Table 1 displays the summarized data for the thermal analysis while Figure 4 shows the weight loss (TG) and derivative curves (dTG) as a function of temperature in nitrogen and air atmosphere, respectively.

Table 1. TGA data of untreated and LbL-treated fabrics in nitrogen and air.

Sample	T_{onset} [°C]	T^*_{max1} [°C]	T^*_{max2} [°C]	Residue at 800°C [%]
Nitrogen				
PET	400	439	-	13.6

5BL	398	440	-	17.4
5BL 0.1M NaCl	398	436	-	19.4
Air				
PET	395	430	537	1.1
5BL	385	440	578	4.1
5BL 0.1M NaCl	395	458	587	6.2

*From derivative curves.

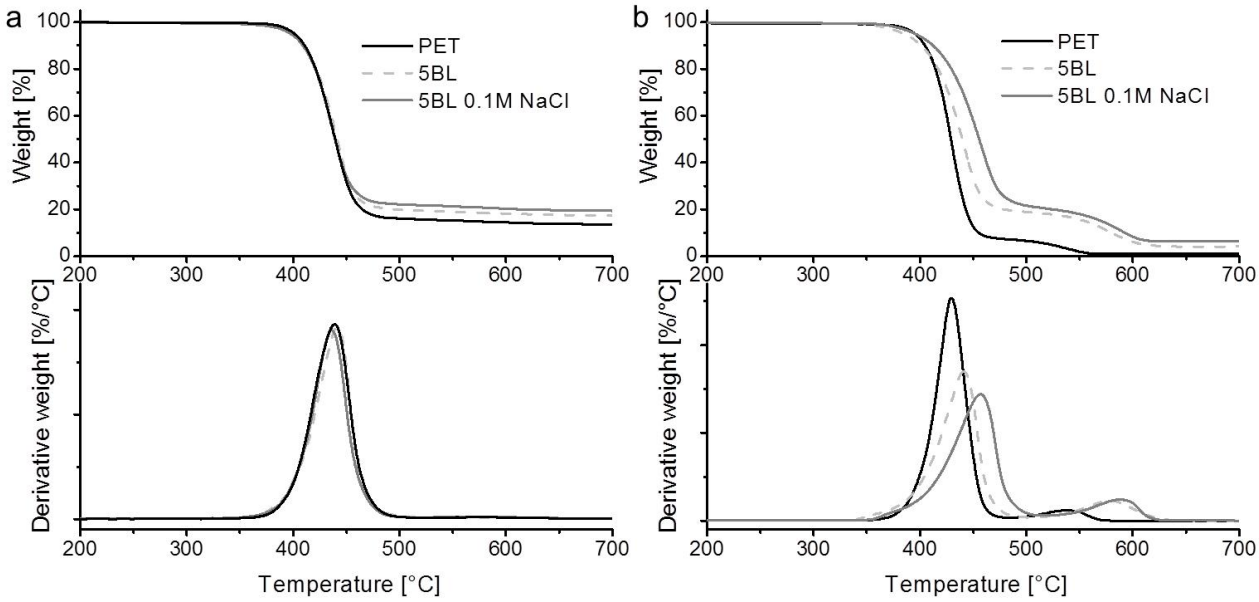

Figure 3. TG and dTG curves of untreated and LbL-treated fabrics in nitrogen (a) and air (b).

In nitrogen, the thermal decomposition of PET takes place in a single within 400 and 500°C and is the result of two competitive processes, namely volatilization and charring; this latter yields a final residue of 13.6 %. [39] The deposition of a LbL coating does not modify the thermal decomposition of PET that still occurs in one step. However, the presence of LbL stratified MMT nanoplatelets improves the char production as pointed out by residue values at 800°C in Table 1. It is worth mentioning that such increase is higher that the calculated coating add-on (1.2 and 2% for 5BL and 5BL 0.1M NaCl, respectively) and thus has to be related to a beneficial effect of the coating in the

PET char production mechanism. Because of a more homogenous and thick coating, 5BL 0.1M NaCl yields the highest final residue increasing the car production by 43%.

In air, neat PET thermal degradation follows two steps. The first occurs between 400 and 500°C and is due to degradation of PET chains into smaller fragments with the production of aliphatic char. [40] The second takes place after 500°C and is related to thermo-oxidative degradation of previously produced char into volatile products.[41] Again, as observed in nitrogen, the presence of the LbL coatings does not affect the degradation mechanism of PET. However, beneficial effects can be detected, especially in the case of 5BL 0.1M NaCl samples. Indeed, all treated fabrics showed an increase in the degradation temperature as noticeable from T_{onset} values. Moreover, the first degradation step occurs at higher temperature and at lower degradation rates as demonstrated by T_{max1} values in Table 2 and a reduced height of the dTG curve in Figure 4 b. The presence of the coating improves the char production that is increased to 20% with respect to the 10% of untreated PET. During the second degradation step, the produced residue is more stable as its thermal oxidation is shifted to higher temperatures (see Tmax2 values in Table 1). Such behavior can be ascribed to the presence of the coating that, as observed in nitrogen can increase the char produced by PET. Moreover, the preferential orientation of MMT nanoplatelets can act as a barrier towards oxygen diffusion during both degradation steps thus postponing and slowing down the oxidation processes. This is more apparent for 5BL 0.1M NaCl. The final residue is 4.1% for 5BL and 6.1% for 5BL 0.1 M NaCl.

Horizontal flame spread test

To evaluate the fire performance of the coated fabric, a flammability test has been performed in horizontal configuration. This test is very important as it evaluates the propensity of the fabric to initiate or propagate the fire when exposed to small flames and it is normally used for the assessment of the fire protection properties of materials. The flammability test results are summarized in Table 2, while Figure 2 in supplementary material reports the snapshots taken during the tests.

Table 2*. Flammability test data of uncoated and LbL coated PET fabrics.*

Sample	Afterflame time [s]	Burning rate [mm/s]	Burns completely	Melt dripping/ Cotton ignition	Mass loss [%]
PET	20 ± 8	6.0 ± 0.2	Yes*	Yes/Yes	64 ± 21*
5BL	35 ± 12	4.2 ± 0.1	Yes	No/Yes**	94 ± 9
5BL 0.1M NaCl	48 ± 1	3.1 ± 0.1	Yes	No/No	94 ± 2
5BL 0.1M NaCl _washed	41±2	2.9 ± 0.4	Yes	No/No	88 ± 3

** Untreated PET displayed vigorous melt dripping that randomly extinguishes the flame; for this reason, the resulting residues are extremely variable.*

*** 20% of samples showed collapsing of flaming big chunk of fabric towards the end of the test*

After ignition, the unmodified PET crumples and loses its shape as the flame propagates along the specimen. During the combustion some flaming droplets are released, this causes the flames on the burning specimen to dwindle and rapidly regrow while spreading on the fabric (see supplementary material Figure 2). The flaming droplets are always able to ignite the cotton placed underneath the sample holder. Sometimes a vigorous dripping may extinguish the flame prior to the complete combustion of the sample. For this reason the values of the final residues are highly variable. It is important to point out that although as a consequence of the melt dripping phenomenon the flame

extinguishes, such behavior is highly undesirable as it can easy spread the fire to other ignitable materials, thus representing one of the most severe fire threats of PET fibers.

LbL coated specimens showed a different flammability behavior: after the removal of the ignition source the flame slowly and constantly propagates on the sample without the formation of molten polymer droplets. In details, 5BL samples do not exhibit melt dripping but rather a collapsing behavior with relatively big parts of detaching from the fabric and falling down igniting the cotton. This was observed for 20% of tested samples. On the other hand 5BL 0.1M NaCl samples can completely suppress the melt dripping phenomenon while achieving the slowest burning rates. These improvements are ascribed to the presence of the coating that can on one hand reduce the volatiles release slowing down the combustion and on the other hand mechanically sustain the fibers thus preventing the formation of the melt dripping phenomenon. This latter effect shows a dependency on the coating morphology as it occurs systematically only for 5BL 0.1M NaCl samples which have been shown to yield the thicker and more homogeneous deposition (see Figure 3 d and f). Thus, in order to perform a preliminary assessment of the coating durability, LbL samples treated at high ionic strength have been washed for 1 hour at 70°C under vigorous stirring and then subjected to horizontal flame spread tests. Figure 5 reports a comparison between FESEM micrographs performed before and after the washing while flame spread tests results are reported in Table 2.

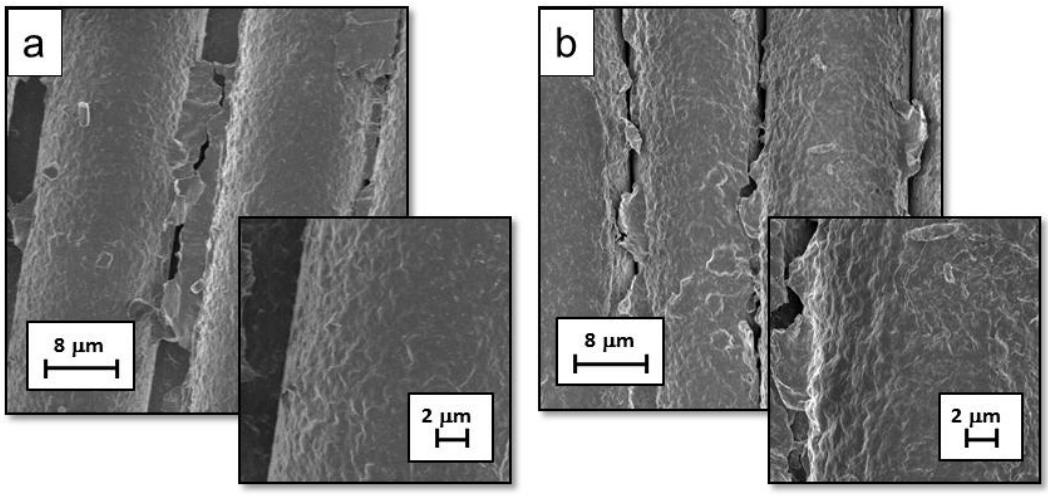

Figure 4. FESEM micrograph of 5BL 0.1M NaCl before (a) and after (b) washing at 70°C for 1 hour.

Unexpectedly, FESEM observations revealed almost no changes in surface morphology for the washed samples that are still able to completely suppress the melt dripping phenomenon and slow down flame propagation during flammability tests as reported in Table 2 and imaged in supplementary material Figure 3. This demonstrates that the deposited coating can survive a washing step without losing effectiveness. Such finding is encouraging as it points out that the deposited LbL coatings have an intrinsic stability which is likely ascribed to the nanoscale electrostatic interactions that holds the coating components together as well as the presence of a surface activation layer made of BPEI. Indeed, this latter component adsorption is expected to be irreversible, [42] thus conferring an overall starting stability to the deposited LbL coating.

Cone calorimetry test

To better evaluate the fire performances of the inorganic coatings, cone calorimetry analyses have been performed. Cone calorimetry is a useful technique for investigating the burning behavior of a material when exposed to an heat flux typical of developing fires (the 35kW/m^2 adopted here represents the initial stage of a fire). [43] During the test, the samples are quickly heated by a radiant heating source; the exposures to the heat flux triggers the thermal degradation reactions in the polymeric phases with subsequent release of volatile and combustible species. At sufficient concentration, such volatiles are ignited by a spark igniter and the flaming combustion of the sample begins. The instrument measures the heat released based on the principle of that the net heat of combustion is proportional to the mass of oxygen required for combustion (13.1 kJ of heat is released per g of oxygen consumed). HRR plots are reported in Figure 6 while the collected cone calorimetry results are summarized in Table 3.

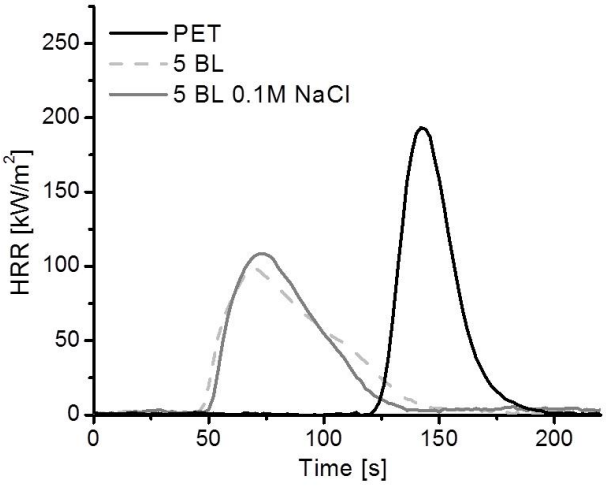

Figure 6 HRR plots of unmodified and LbL treated PET fabrics.

Table 3. Cone calorimetry data of unmodified and LbL treated PET fabrics.

Sample	**TTI ±σ [s]**	**pkHRR ±σ [kW/m^2]**	**THR ±σ [MJ/m^2]**	**TSR ±σ [m^2/m^2]**	**Residue ±σ [%]**
Reference	106±12	202 ± 22	5.2 ± 0.1	171 ± 20	5 ± 1
5 BL	51±4	102 ± 7	5.3 ± 0.1	182 ± 2	11 ± 1
5 BL 0.1M NaCl	50±20	107 ± 2	5.1 ± 0.2	175 ± 17	12 ± 1

Unmodified PET fabrics ignite after an average 106 seconds burning with a vigorous flame and reaching a pkHRR of 202 kW/m^2. The presence of the LbL coating, regardless of the adopted ionic strength, strongly modifies the burning behavior of the PET as reported in Figure 6. Indeed, all LbL treated samples showed an anticipation in TTI values that are reduced by 53%. Despite of this, the heat release rate is massively reduced as demonstrated by pkHRR values reported in Table 3 (202 vs 102 and 107 kW/m^2 for PET, 5BL and %B 0.1M Nacl, respectively). A similar behavior has been reported before for bulk clay nanocomposites and, although some theories have been proposed, the real explanation is yet to be reported.[44] However, what appears to be consolidated is that the presence of clay can on one hand lead to TTI anticipation in the pre-ignition phase and on the other

hand substantially reduce the combustion kinetics. This latter effect is related to the clay that builds up an inorganic barrier made of nanoplatelets preferentially laying flat on the surface of the burning material. As a consequence, the mass transfer that from the bulk feeds the flame with flammable volatiles is limited. A similar behavior is expected to control the burring behavior of LbL treated PET fabrics; indeed, as reported in Figure 3, each fiber is conformally coated with stratified MMT nanoplatelets intercalated by POSS. The deposited coating can thus exert the function of protective barrier from the very beginning of the combustion greatly slowind down the combustion kinetics as demonstrated by the different shape of HRR plots between unmodified and LbL treated PET (Figure 6). This is also corroborated by the residues collected at the end of the test (Figure S): unmodified PET yields a mass of molten charred polymer (5% of the original mass) while LbL treated samples show a coherent and compact residue (11 and 12 % for 5BL and 5BL 0.1M NaCl, respectively). Finally, the presence of the coating does not affect the smoke production as demonstrated by the nearly identical TSR values reported in Table 3.

Conclusions

This work presented the Layer by Layer assembly of inorganic coatings made of POSS and MMT on PET fabric employing a semi industrial approach and investigating the effects of ionic strength on the achieved flame retardancy properties. Coating growth characterization performed with infrared spectroscopy demonstrated that the POSS/MMT pair can yield a steady linear build up. The inclusion of NaCl in the process deeply influences the coating growth by modifying the ionic strength of the systems thus resulting in thicker coatings. 0.1 M NaCl is found to promote the highest adsorption at each deposition step. The POSS/MMT systems at zero and high ionic strength were then successfully deposited on PET fabrics employing a dyeing padder in a impregnation and exhaustion process thus demonstrating the viability of LbL processes at modified ionic strength in a semi industrial approach. Coatings deposited at high ionic strength are thicker and more homogeneous than their unmodified counterparts as assessed by FESEM and ATR analyses. This

difference in morphology is found to play a key role in the achieved performances. Indeed, coatings deposited at 0.1M NaCl achieved the best thermal stability and flame retardancy properties. The melt dripping was completely suppressed and the burning rate significantly reduced during horizontal flame spread tests. Surprisingly, these performances were maintained after 1 hour washing at 70°C. This finding was also confirmed by FESEM observation and demonstrates that the coatings possess an inherent stability that could be further ameliorated by the use of crossing strategies such as UV curing. By cone calorimetry treated fabrics showed a strong reduction in the combustion kinetics by nearly halving the peak of heat release rate. The flame retardancy mechanism of the coating is identified as a condensed phase one. Highly oriented MMT nanoplatelets intercalated by POSS can exert a barrier function slowing down the mass transfer of combustible volatiles towards the flame. In conclusion, the presented LbL coatings demonstrate good fire performance, with a simple productive process and a good reproducibility. Further improvements can exploit the inclusion of gas phase flame retardants searching for synergic effects. The approach described in this paper provides additional information on the viability of tuning ionic strength when depositing LbL coatings on fabrics employing industrial-like processes thus enabling for a further step towards high efficient and green fire protection solutions to be exploited and extended to several substrates.

Acknowledgements

The authors want to thank Mr. Mauro Raimondo and Dr. Fabio Cuttica for FESEM imaging and cone Calorimetric Analysis, respectively.

References

1. Aizenshtein, E., Polyester fibres continue to dominate on the world textile raw materials balance sheet. *Fibre chemistry* **2009,** *41* (1), 1-8.

2. Alongi, J.; Ra, H.; Carosio, F.; Malucelli, G., *Update on flame retardant textiles: state of the art, environmental issues and innovative solutions*. Smithers Rapra Technology Ltd: 2013.

3. Birnbaum, L. S.; Staskal, D. F., Brominated Flame Retardants: Cause for Concern? *Environmental Health Perspectives* **2003,** *112* (1), 9-17.

4. Xiao, H.; Shen, L.; Su, Y.; Barresi, E.; Dejong, M.; Hung, H.; Lei, Y. D.; Wania, F.; Reiner, E. J.; Sverko, E.; Kang, S. C., Atmospheric concentrations of halogenated flame retardants at two remote locations: the Canadian High Arctic and the Tibetan Plateau. *Environmental pollution* **2012,** *161*, 154-61.

5. Barcelo, D.; Kostianoy, A. G., Handbook environmental chemistry. In *Brominated flame retardants*, Heidelberg, S.-V. B., Ed. 2011; Vol. 16.

6. Malucelli, G.; Carosio, F.; Alongi, J.; Fina, A.; Frache, A.; Camino, G., Materials engineering for surface-confined flame retardancy. *Mat Sci Eng R* **2014,** *84*, 1-20.

7. Alongi, J.; Carosio, F.; Malucelli, G., Current emerging techniques to impart flame retardancy to fabrics: An overview. *Polym Degrad Stabil* **2014,** *106*, 138-149.

8. Fina, A.; Camino, G., Ignition mechanisms in polymers and polymer nanocomposites. *Polymers for Advanced Technologies* **2011,** *22* (7), 1147-1155.

9. Alongi, J.; Bosco, F.; Carosio, F.; Di Blasio, A.; Malucelli, G., A new era for flame retardant materials? *Mater Today* **2014,** *17* (4), 152-153.

10. Carosio, F.; Di Blasio, A.; Alongi, J.; Malucelli, G., Green DNA-based flame retardant coatings assembled through Layer by Layer. *Polymer* **2013,** *54* (19), 5148-5153.

11. Carosio, F.; Cuttica, F.; Di Blasio, A.; Alongi, J.; Malucelli, G., Layer by layer assembly of flame retardant thin films on closed cell PET foams: Efficiency of ammonium polyphosphate versus DNA. *Polymer Degradation and Stability* **2015,** *113*, 189-196.

12. Patra, D.; Vangal, P.; Cain, A. A.; Cho, C.; Regev, O.; Grunlan, J. C., Inorganic Nanoparticle Thin Film that Suppresses Flammability of Polyurethane with only a Single Electrostatically-Assembled Bilayer. *Acs Appl Mater Inter* **2014,** *6* (19), 16903-16908.

13. Carosio, F.; Alongi, J., Ultra-Fast Layer-by-Layer Approach for Depositing Flame Retardant Coatings on Flexible PU Foams within Seconds. *Acs Appl Mater Inter* **2016,** *8* (10), 6315-6319.

14. Wang, X.; Pan, Y.-T.; Wan, J.-T.; Wang, D.-Y., An eco-friendly way to fire retardant flexible polyurethane foam: layer-by-layer assembly of fully bio-based substances. *Rsc Adv* **2014,** *4* (86), 46164-46169.

15. Carosio, F.; Di Blasio, A.; Alongi, J.; Malucelli, G., Layer by layer nanoarchitectures for the surface protection of polycarbonate. *European Polymer Journal* **2013,** *49* (2), 397-404.

16. Apaydin, K.; Laachachi, A.; Ball, V.; Jimenez, M.; Bourbigot, S.; Toniazzo, V.; Ruch, D., Polyallylamine-montmorillonite as super flame retardant coating assemblies by layer-by layer deposition on polyamide. *Polym Degrad Stabil* **2013,** *98* (2), 627-634.

17. Galeska, I.; Hickey, T.; Moussy, F.; Kreutzer, D.; Papadimitrakopoulos, F., Characterization and Biocompatibility Studies of Novel Humic Acids Based Films as Membrane Material for an Implantable Glucose Sensor. *Biomacromolecules* **2001,** (2), 7.

18. Rao, S. V.; Anderson, K. W.; Bachas, L. G., Controlled Layer-By-Layer Immobilization of Horseradish Peroxidase. *Biotechnology And Bioengineering* **1999,** *65* (4), 8.

19. Zahr, A. S.; Villiers, M. d.; Pishko, M. V., Encapsulation of Drug Nanoparticles in Self-Assembled Macromolecular Nanoshells. *Langmuir* **2005,** (21), 8.

20. Sukhorukov, G. B.; Mohwald, H., Multifunctional cargo systems for biotechnology. *Trends in biotechnology* **2007,** *25* (3), 93-8.

21. Billingham, J.; C.Breen; J.Harwood, Adsorption of polyamine, polyacrylic acid and polyethylene glycol on montmorillonite: An in situ study using ATR-FTIR. *Vibrational Spectroscopy* **1997,** *14*, 15.

22. R.K.Iler, Multilayers of Colloidal Particles. *Journal of colloid and interface science* **1966,** *21*, 26.

23. Decher, G.; Hong, J. D.; Schmitt, J., Buildup of ultrathin multilayer films by a self-assembly process: III. Consecutively alternating adsorption of anionic and cationic polyelectrolytes on charged surfaces. *Thin Solid Films* **1992,** *210*, 5.

24. Decher, G., Fuzzy nanoassemblies: Toward layered polymeric multicomposites. *Science* **1997,** *277* (5330), 1232-1237.

25. Berndt, P.; Kurihara, K.; Kunitake, T., Adsorption of poly(styrenesulfonate) onto an ammonium monolayer on mica: a surface forces study. *Langmuir* **1992,** *8* (10), 2486-2490.

26. Bergbreiter, D. E.; Tao, G.; Franchina, J. G.; Sussman, L., Polyvalent Hydrogen-Bonding Functionalization of Ultrathin Hyperbranched Films on Polyethylene and Gold. *Macromolecules* **2001,** *34* (9), 3018-3023.

27. Sun, J.; Wu, T.; Liu, F.; Wang, Z.; Zhang, X.; Shen, J., Covalently Attached Multilayer Assemblies by Sequential Adsorption of Polycationic Diazo-Resins and Polyanionic Poly(acrylic acid). *Langmuir* **2000,** *16* (10), 4620-4624.

28. Shimazaki, Y.; Mitsuishi, M.; Ito, S.; Yamamoto, M., Preparation of the Layer-by-Layer Deposited Ultrathin Film Based on the Charge-Transfer Interaction. *Langmuir* **1997,** *13* (6), 1385-1387.

29. Carosio, F.; Negrell-Guirao, C.; Di Blasio, A.; Alongi, J.; David, G.; Camino, G., Tunable thermal and flame response of phosphonated oligoallylamines layer by layer assemblies on cotton. *Carbohydrate polymers* **2015,** *115*, 752-759.

30. McAloney, R. A.; Sinyor, M.; Dudnik, V.; Goh, M. C., Atomic force microscopy studies of salt effects on polyelectrolyte multilayer film morphology. *Langmuir* **2001,** *17* (21), 6655-6663.

31. Guin, T.; Krecker, M.; Milhorn, A.; Hagen, D. A.; Stevens, B.; Grunlan, J. C., Exceptional Flame Resistance and Gas Barrier with Thick Multilayer Nanobrick Wall Thin Films. *Advanced Materials Interfaces* **2015,** *2* (11).

32. Nolte, A. J.; Takane, N.; Hindman, E.; Gaynor, W.; Rubner, M. F.; Cohen, R. E., Thin Film Thickness Gradients and Spatial Patterning via Salt Etching of Polyelectrolyte Multilayers. *Macromolecules* **2007,** *40*, 8.

33. Carosio, F.; Alongi, J., Influence of layer by layer coatings containing octapropylammonium polyhedral oligomeric silsesquioxane and ammonium polyphosphate on the thermal stability and flammability of acrylic fabrics. *J Anal Appl Pyrol* **2016,** *119*, 114-123.

34. Cain, A. A.; Plummer, M. G. B.; Murray, S. E.; Bolling, L.; Regev, O.; Grunlan, J. C., Iron-containing, high aspect ratio clay as nanoarmor that imparts substantial thermal/flame protection to polyurethane with a single electrostatically-deposited bilayer. *J Mater Chem A* **2014,** *2* (41), 17609-17617.

35. Hoogeveen, N. G.; Cohen Stuart, M. A.; Fleer, G. J.; Böhmer, M. R., Formation and stability of multilayers of polyelectrolytes. *Langmuir* **1996,** *12* (15), 3675-3681.

36. Tata, J.; Alongi, J.; Carosio, F.; Frache, A., Optimization of the procedure to burn textile fabrics by cone calorimeter: Part I. Combustion behavior of polyester. *Fire Mater* **2011,** *35* (6), 397-409.

37. Zhang, Z.; Liang, G.; Lu, T., Synthesis and characterization of cage octa (aminopropylsilsesquioxane). *J Appl Polym Sci* **2007,** *103* (4), 2608-2614.

38. Madejová, J., FTIR techniques in clay mineral studies. *Vibrational spectroscopy* **2003,** *31* (1), 1-10.

39. Alongi, J.; Camino, G.; Malucelli, G., Heating rate effect on char yield from cotton, poly(ethylene terephthalate) and blend fabrics. *Carbohydrate polymers* **2013,** *92* (2), 1327-1334.

40. Martın-Gullon, I.; Esperanza, M.; Font, R., Kinetic model for the pyrolysis and combustion of poly-(ethylene terephthalate)(PET). *J Anal Appl Pyrol* **2001,** *58*, 635-650.

41. Wang, X.-S.; Li, X.-G.; Yan, D., Thermal decomposition kinetics of poly (trimethylene terephthalate). *Polym Degrad Stabil* **2000,** *69* (3), 361-372.

42. Szilagyi, I.; Trefalt, G.; Tiraferri, A.; Maroni, P.; Borkovec, M., Polyelectrolyte adsorption, interparticle forces, and colloidal aggregation. *Soft Matter* **2014,** *10* (15), 2479-2502.

43. Schartel, B.; Hull, T. R., Development of fire-retarded materials—Interpretation of cone calorimeter data. *Fire Mater* **2007,** *31* (5), 327-354.

44. Fina, A.; Cuttica, F.; Camino, G., Ignition of polypropylene/montmorillonite nanocomposites. *Polym Degrad Stabil* **2012,** *97* (12), 2619-2626.